Study of the Reaction Stages and Kinetics of the Europium Oxide Carbochlorination

FEDERICO J. POMIRO, GASTÓN G. FOUGA, JUAN P. GAVIRÍA, and ANA E. BOHÉ

The europium oxide (Eu_2O_3(s)) chlorination reaction with sucrose carbon was studied by thermogravimetry between room temperature and 1223 K (950 °C). The nonisothermal thermogravimetry showed that the reaction consists of three stages, and their stoichiometries were studied. The product of the first stage was europium oxychloride, and it showed independence of the reaction kinetics with the carbon content. Subsequently, in the second stage, the EuOCl(s) was carbochlorinated with formation of $EuCl_3$(l) and its evaporation is observed in the third stage. The analysis by Fourier transform infrared spectroscopy of gaseous species showed that the reaction at second stage occurs with the formation of CO_2(g) and CO(g). Both reactants and products were analyzed by X-ray diffraction, scanning electron microscopy and wavelength-dispersive X-ray fluorescence spectroscopy. The influence of carbon content, total flow rate, sample initial mass, chlorine partial pressure, and temperature were evaluated. The second stage kinetics was analyzed, which showed an anomalous behavior caused by generation of chlorine radicals during interaction of Cl_2(g) and carbon. It was found that the reaction rate at 933 K (660 °C) was proportional to a potential function of the chlorine partial pressure whose exponent is 0.56. The conversion curves were analyzed with the Avrami-Erofeev model and it was obtained an activation energy of 154 ± 5 kJ mol^{-1}.

DOI: 10.1007/s11663-014-0196-7

I. INTRODUCTION

THE rare earths play an important role in many fields of advanced materials for high technology. In this context, it is very important to study methods of extraction for these elements.[1–3]

The chlorination and carbochlorination of metallic oxides are very important processes in the industrial production of pure metals. This method is economic and efficient compared with wet extraction processes. It is well known that chlorine possesses a high reactivity toward many compounds at a relatively low temperature.[4–7] Many metallic oxides can be transformed to metals through a process that consists of three stages. In the first, the carbochlorination stage, the oxide reacts with chlorine in presence of carbon to produce the metallic chloride. Subsequently, the metal is obtained from the reduction of the chloride. Finally, the metallic sponge is purified by high-temperature vacuum distillation.[8–11]

The carbochlorination at 1273 K and 1473 K (1000 °C and 1200 °C) with Cl_2(g) and carbon has been applied industrially for bastnaesite concentrate ((Ce,La,Nd)(CO_3)F).[12] Gimenes and Oliveira studied the reaction among xenotime (YPO_4), chlorine, and carbon, and a global rate equation was developed.[13] The rare earth chlorides mixtures obtained by carbochlorination of rare earth minerals with Cl_2(g) can be separated using chemical-vapor transport (CVT) mediated by the formation of volatile complexes with KCl and $AlCl_3$.[14,15]

The carbochlorination of the Y_2O_3(s),[10,11] Sm_2O_3(s),[16] and CeO_2(s)[17] with carbon as a reductant and chlorine gas as a chlorination agent has been reported by other authors, but the carbochlorination of Eu_2O_3(s) has not been studied. In a work recently published we have studied the chlorination reaction of europium oxide. The formation of EuOCl(s) like reaction product at temperatures above 523 K (250 °C) was determined. The EuOCl(s) is further chlorinated to europium trichloride at temperatures above 1123 K (850 °C). The chloride has a considerable vapor pressure, and the evaporation rate is higher than its production rate.[18]

The objective of this work is to elucidate the reaction stages of the Eu_2O_3(s) carbochlorination, and study the stoichiometry and kinetics of each stage.

FEDERICO J. POMIRO, Researcher, is with the Departamento de Fisicoquímica y Control de Calidad, Complejo Tecnológico Pilcaniyeu, Centro Atómico Bariloche, Comisión Nacional de Energía Atómica, Av. Bustillo 9500, 8400 S.C. de Bariloche, Río Negro, Argentina. Contact e-mail: pomiro@cab.cnea.gov.ar GASTÓN G. FOUGA and JUAN P. GAVIRÍA, Assistant Professors, are with the Departamento de Fisicoquímica y Control de Calidad, Complejo Tecnológico Pilcaniyeu, Centro Atómico Bariloche, Comisión Nacional de Energía Atómica, and also with the Consejo Nacional de Investigaciones Científicas y Técnicas (CONICET), Argentina, Av. Rivadavia 1917, 1033 Ciudad Autónoma de Buenos Aires, Buenos Aires, Argentina. ANA E. BOHÉ, Professor, is with the Departamento de Fisicoquímica y Control de Calidad, Complejo Tecnológico Pilcaniyeu, Centro Atómico Bariloche, Comisión Nacional de Energía Atómica, also with the Consejo Nacional de Investigaciones Científicas y Técnicas (CONICET), Argentina, and also with the Centro Regional Universitario Bariloche, Universidad Nacional del Comahue, Quintral 1250, 8400 S.C. de Bariloche, Río Negro, Argentina.

Manuscript submitted April 11, 2014.
Article published online October 15, 2014.

II. MATERIALS AND METHODS

The gases used were Cl_2(g) 99.8 pct purity (Praxair, Buenos Aires, Argentina) and Ar(g) 99.99 pct purity (LINDE, Buenos Aires, Argentina). The solid starting reactant was Eu_2O_3(s) 99.99 pct purity (Sigma-Aldrich Chemical Company Inc., St. Louis, MO) and sucrose carbon obtained from the pyrolysis of sucrose (Fluka Chemical AG, St. Louis, MO) in inert atmosphere at 1253 K (980 °C) during 48 hours and sieved to a size of 400 mesh (ASTM, square aperture of 37 μm). The carbon characteristics were described by Gonzalez *et al.*[19] Respective amounts of the solids reactants were weighed and mixed mechanically to obtain mixtures of Eu_2O_3(s)-carbon in the range of 3 to 10 pct (carbon mass/total mass).

Initial reactants were previously characterized by scanning electron microscopy (SEM 515; Philips XL30 Electronics Instruments, Amsterdam, The Netherlands), X-ray diffraction (XRD, Bruker D8 Advance; Bruker Corporation, Karlsruhe, Germany), with Ni filtered and Cu K_α radiation and multielement analysis was carried out by wavelength-dispersive X-ray fluorescence spectroscopy (WD-XRF, Bruker S8 Tiger; Bruker Corporation, Karlsruhe, Germany).

Figure 1 shows the diffractogram of the starting sample with the reference pattern (Ref. 431008).[20] By comparing the positions and intensities of the diffraction peaks, it can be concluded that the starting sample is composed by a simple phase of Eu_2O_3(s), which crystallizes in the cubic system (space group *Ia*3).

Figure 2 shows SEM images of Eu_2O_3(s)-C mixtures. These micrographs show an average particle size of 2 to 5 μm (Figure 2(a)) and 20 to 30 μm (Figure 2(b)) for Eu_2O_3(s) and carbon, respectively.

Mass changes occurring during Eu_2O_3(s) carbochlorination reaction were measured using a high-resolution thermogravimetric analyzer (TGA). It consists of an electrobalance (model 2000, Cahn Instruments Inc.), a vertical tube furnace, a gas line and a data acquisition system. This experimental setup has a sensitivity of ± 5 μg under a gas flow rate between 2 and 8 L h^{-1} (measured under normal conditions of temperature and pressure) in the range from room temperature to 1273 K (1000 °C). Each sample was placed in a cylindrical silica glass crucible (diameter = 0.72 cm, high = 0.42 cm), which hangs from one of the arms of the electrobalance through a silica glass wire. The temperature of the sample was measured using a Pt-Pt (10 pct Rh) thermocouple encapsulated in silica glass, which was placed 2 mm below the crucible. Flows of Ar(g) and Cl_2(g) gases were controlled by means of flowmeters. Nonisothermal and isothermal runs were performed. In the nonisothermal run, the Cl_2(g) was introduced and the samples were heated in the resulting mixture Cl_2(g)-Ar(g) from room temperature to 1223 K (950 °C). In the isothermal runs, the samples were heated in flowing Ar until the reaction temperature was reached. Once the temperature was stabilized, chlorine was admitted into the hangdown tube while the mass changes were continuously monitored. Relative mass changes monitored were acquired every second using a data acquisition system (network data acquisition and control modules, model DB-1820, ICP DAS USA Inc., Lomita) with the experimental setup described above.

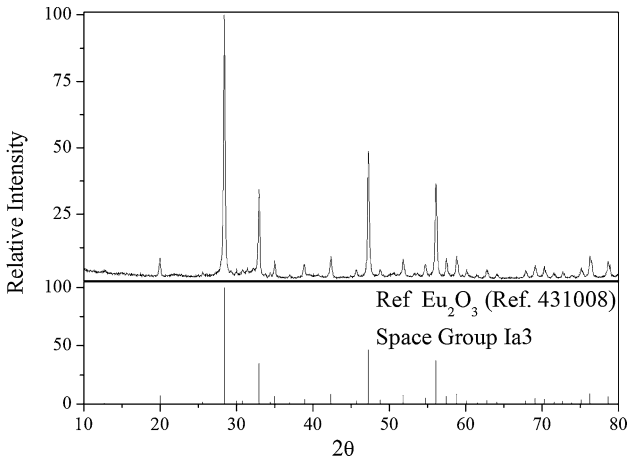

Fig. 1—XRD patterns for the starting reactant and the Eu_2O_3(s) reference.

The gas species were identified by Fourier transform infrared spectroscopy (FTIR, PerkinElmer Spectrum 400; PerkinElmer, Waltham, MA). The carbochlorination reactions for these identifications were performed in a fixed bed reactor. The reactor consists of a horizontal silica glass tube and the sample was placed in a silica glass crucible. The gases at the outlet of the reactor can be conducted to the purge or to a gas cell sealed with sodium chloride windows. This cell is removed and subsequently analyzed by FTIR.

III. THERMODYNAMIC CONSIDERATIONS

The following reactions are possible in the Eu_2O_3(s)-C(s)-Cl_2(g) system:

$$Eu_2O_3(s) + Cl_2(g) + C(s) \rightarrow 2EuOCl(s) + CO(g), \quad [1]$$

$$1/3Eu_2O_3(s) + Cl_2(g) + C(s) \rightarrow 2/3EuCl_3(s,l) + CO(g), \quad [2]$$

$$Eu_2O_3(s) + Cl_2(g) + 1/2C(s) \rightarrow 2EuOCl(s) + 1/2CO_2(g), \quad [3]$$

$$1/3Eu_2O_3(s) + Cl_2(g) + 1/2C(s) \rightarrow 2/3EuCl_3(s,l) + 1/2CO_2(g), \quad [4]$$

$$Eu_2O_3(s) + Cl_2(g) \rightarrow 2EuOCl(s) + 1/2O_2(g), \quad [5]$$

$$1/3Eu_2O_3(s) + Cl_2(g) \rightarrow 2/3EuCl_3(s,l) + 1/2O_2(g). \quad [6]$$

The physical properties reported for europium compounds are as follows: EuO [T_m = 1973 K (1700 °C)][21]; Eu_2O_3 [T_m = 2623 K (2350 °C)], [T_b = 4063 K

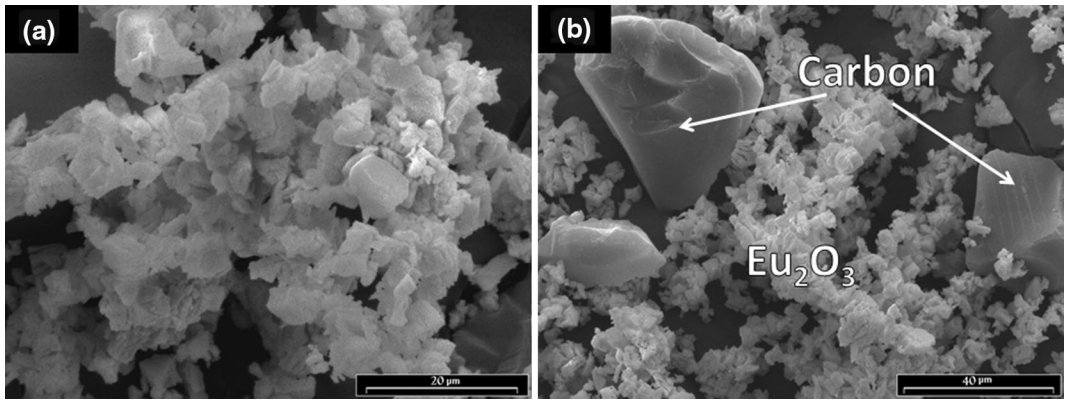

Fig. 2—SEM images of (*a*) Eu_2O_3(s) and (*b*) Eu_2O_3(s)-carbon mixture.

(3790 °C)][21]; EuOCl [T_d = 1673 K (1400 °C) (in vacuum)][22]; $EuCl_2$ [T_m = 1004 K (731 °C), T_b = 2335 K (2062 °C)][23]; $EuCl_3$ [T_m = 896 K (623 °C), [21] 894 K (621 °C)],[24] T_b = [1891 K (1618 °C)[21]]. T_m, T_d, and T_b are the melting, decomposition and boiling temperatures.

The formation of Eu^{2+} compounds were not considered because of the presence of a highly oxidative atmosphere of chlorine. It is well known that the carbon is a reductant agent, so the possible interaction between Eu_2O_3(s) and sucrose carbon was analyzed. This study was carried out by thermogravimetry at 1223 K (950 °C) in argon atmosphere for 6 hours and no mass changes were observed; the XRD analysis of the final solid did not show chemical changes. This result is in accord with the high positive value reported for the reduction of the oxide by carbon with formation of EuO(s) and CO(g) ($\Delta G°$: 184 and 108 kJ mol^{-1} for 873 K and 1273 K [600 °C and 1000 °C], respectively).[25]

The dismutation reaction of EuOCl(s) forming $EuCl_3$(s,l) and Eu_2O_3(s) is not considered because it has a positive value of $\Delta G°$ at the range of temperature used in this work[18] [$\Delta G°$: 34 and 24 kJ mol^{-1} for 873 K and 1273 K (600 °C and 1000 °C), respectively].[25]

Figure 3 shows the standard Gibbs free energy for the above Reactions [1] through [6]. The thermodynamic calculations were performed using the HSC chemistry 6.1 software for windows.[25]

The results of the thermodynamic calculations indicate that EuOCl(s) can be produced in a first stage by Reactions [1], [3], and [5]. The formation of oxychloride has the most negative $\Delta G°$ values and is thermodynamically more feasible to occur than the formation of europium trichloride. Then, the EuOCl(s) can react through the following reactions:

$$EuOCl(s) + Cl_2(g) \rightarrow EuCl_3(s,l) + 1/2O_2(g), \quad [7]$$

$$EuOCl(s) + Cl_2(g) + 1/2C(s) \rightarrow EuCl_3(s,l) + 1/2CO_2(g), \quad [8]$$

$$EuOCl(s) + Cl_2(g) + C(s) \rightarrow EuCl_3(s,l) + CO(g) \quad [9]$$

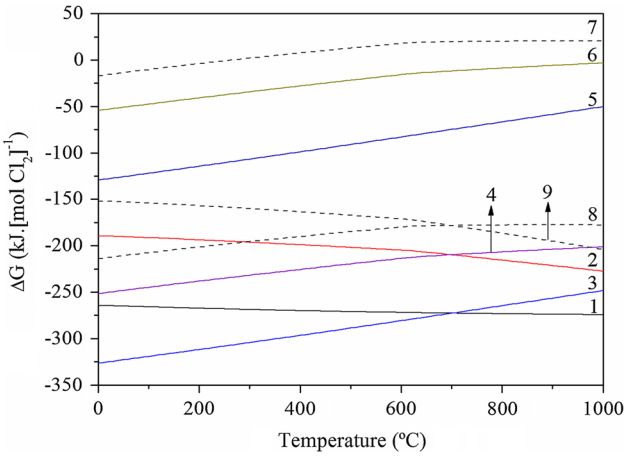

Fig. 3—Ellingham diagram for the reactions involved in the Eu_2O_3(s)-C(s)-Cl_2(g) system.

The standard Gibbs free energy for Reactions [7] through [9] are shown in Figure 3. Reaction [7] has positive values of $\Delta G°$ for $T > 523$ K (250 °C). The curves show that the Reactions [8] and [9] have negative $\Delta G°$ values, indicating that they are thermodynamically favorable. The oxychloride carbochlorination with formation of CO_2(g) has the most negative $\Delta G°$ values below 973 K (700 °C), so it is thermodynamically more feasible to occur at these temperatures. Reaction [9] has lower $\Delta G°$ values at temperatures higher than 973 K (700 °C). The curves associated with the $EuCl_3$ formation through Reactions [8] and [9] in the presence of the reducing agent cross each other at 973 K (700 °C), the same temperature where the curves corresponding to the formation of CO(g) and CO_2(g) have the same Gibbs energy value. This behavior is caused by the Boudouard reaction:

$$CO_2(g) + C(s) \rightarrow 2CO(g). \quad [10]$$

Reaction [10] has positive values of $\Delta G°$ for temperatures lower than 973 K (700 °C); it is equal to zero at 973 K (700 °C) and has negative values for temperatures above 973 K (700 °C).[25]

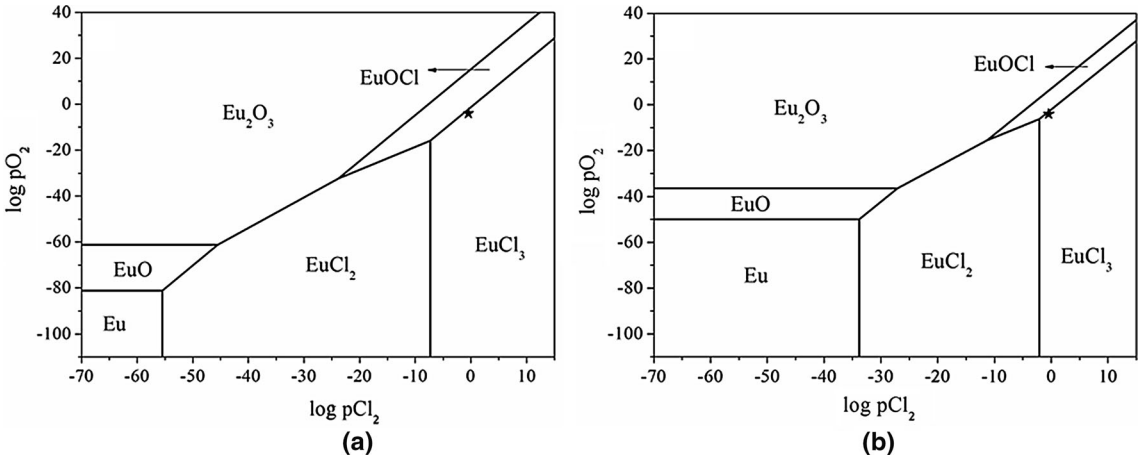

Fig. 4—Phase stability diagrams of Eu-Cl-O system at (*a*) 673 K (400 °C) and (*b*) 1023 K (750 °C). The experimental conditions are indicated with an asterisk.

Figures 4(a) and (b) show the phase stability diagrams of Eu-Cl-O system at [673 K and 1023 K (400 °C and 750 °C)], respectively.[25] The axes of the diagrams are the logarithms of the partial pressure of O_2(g) and Cl_2(g). At the beginning of the chlorination reactions, the values of partial pressure of Cl_2(g) and O_2(g) were 0.35 and 10^{-4} atm, respectively, and these are indicated by an asterisk. The O_2(g) is present in Ar(g) as an impurity. The possible stable condensed phases are Eu(s), EuO(s), Eu_2O_3(s), EuOCl(s), $EuCl_2$(s,l), and $EuCl_3$(s,l). The phase stability diagrams shows that there is not a thermodynamic equilibrium between Eu_2O_3(s) and $EuCl_3$(s,l) at 673 K and 1023 K (400 °C and 750 °C). Therefore, EuOCl(s) has to be formed prior to the formation of $EuCl_3$(s,l) from Eu_2O_3(s).

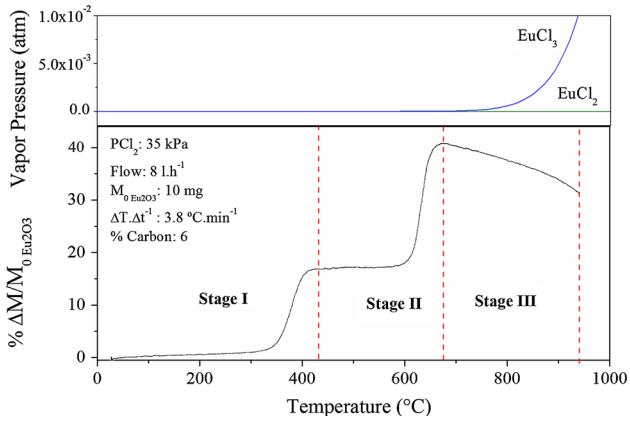

Fig. 5—TG curve for nonisothermal carbochlorination of Eu_2O_3(s) and vapor pressure of $EuCl_3$ and $EuCl_2$.

IV. RESULTS AND DISCUSSION

A. *Nonisothermal Carbochlorination Reaction*

Figure 5 shows the relative sample mass change as a function of temperature between room temperature and 1223 K (950 °C). TG data is expressed as the fractional oxide mass loss given by percent pct $\Delta M/M_{0Eu_2O_3}$, where ΔM is the mass change and $M_{0Eu_2O_3}$ is the initial Eu_2O_3(s) mass in the Eu_2O_3(s)-C(s) mixture. The experimental conditions were: a linear heating rate of 3.8 °C min^{-1}; PCl_2 = 35 kPa, Cl_2(g)-Ar(g) flow = 8 L h^{-1}, $M_{0Eu_2O_3}$ = 10 mg, and percent carbon = 6.

The nonisothermal carbochlorination of Eu_2O_3(s) showed that the reaction consists of three stages. The reaction starts at approximately 523 K (250 °C), showing a sharp mass increase until the mass change reaches a value of pct $\Delta M/M_{0Eu_2O_3}$ = 15.6 at 698 K (425 °C), coinciding with the relative mass change expected for Reaction [5]. This condition is referred to as stage I. From 698 K to 848 K (425 °C to 575 °C) mass change is not observed. The relative mass change increases until a value of 40 pct between 873 K and 943 K (600 °C and 670 °C). This part of the carbochlorination reaction is called stage II. For temperatures above 943 K (670 °C), after stage II, the nonisothermal curve proceeds with mass loss. The vapor pressure curves of europium chlorides are shown in Figure 5.[25] The mass loss observed at temperatures above 943 K (670 °C) is referred as stage III.

B. *Isothermal Experiments*

1. *Analysis at 673 K (400 °C): contribution to the study of stage I*

In order to determinate the products of reaction, stoichiometry and kinetics of Stage I experiments were performed at 673 K (400 °C) and different percentages of carbon: 0, 6 and 10 pct. The experimental conditions were: PCl_2 = 35 kPa, Cl_2(g)-Ar(g) flow = 4 L h^{-1}; and $M_{0Eu_2O_3}$ = 10 mg. Figure 6 shows $\Delta M/M_{0Eu_2O_3}$ *vs t* curves for these experiments. The TG showed a mass increase until the change reaches a value of ΔM $M_{0Eu_2O_3}$ = 0.155, which coincides with the relative mass change of Reaction [5]. This result indicates that the carbon is not consumed because the values of $\Delta M/M_{0Eu_2O_3}$ expected for Reaction [3] (with formation of CO_2) and Reaction [1] (with formation of CO) are 0.14 and 0.13, respectively.

Besides, Figure 6 shows that the reaction rate is unaffected by carbon content.

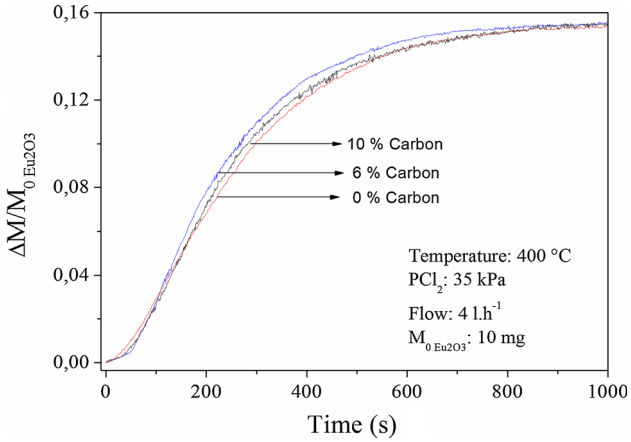

Fig. 6—Influence of carbon content in the chlorination of Eu_2O_3(s) at 673 K (400 °C).

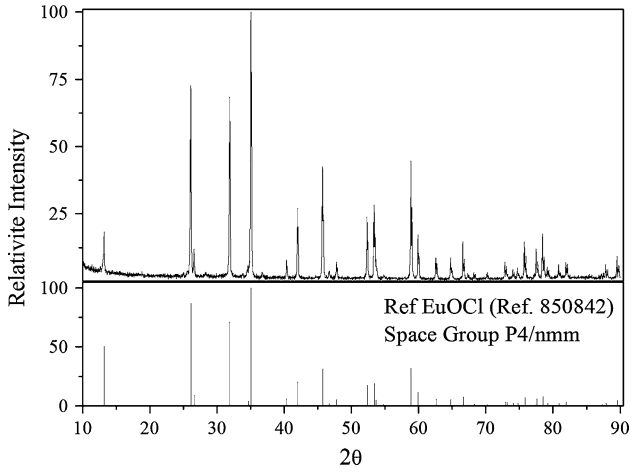

Fig. 7—XRD patterns of the product of Eu_2O_3(s) carbochlorination at 673 K (400 °C), and the EuOCl(s) reference.

The solid product was characterized by SEM and XRD. Figure 7 shows the XRD pattern obtained in which a good agreement is achieved with the corresponding reference pattern for the europium oxychloride also shown in the figure.[20] The analysis performed by WD-XRF of the solid residue was consistent with the chemical formula of EuOCl(s). Figure 8 shows SEM images of the solid residue after reaction at 673 K (400 °C). The SEM image of Figure 8(a) shows an unreacted carbon, which has completely smooth surfaces. Figure 8(b) shows that the EuOCl(s) particles have a size of 2 to 5 μm, which form agglomerates of several microns.

Therefore, the results indicate that the reaction which is taking place in stage I is Reaction [5].

In a work recently published, we have studied the kinetics of the chlorination reaction of Eu_2O_3(s) and the following overall rate equation for the reaction of Eu_2O_3(s) with Cl_2(g), between 573 K and 673 K (300 °C and 400 °C), was obtained:[18]

$$\text{Rate } [s^{-1}] = \frac{d\alpha}{dt} = 3.6 \times 10^5 [s\,kPa^{0.54}]^{-1} \times e^{-(115\,kJ\cdot mol^{-1})/RT} \times (PCl_2[kPa])^{0.54} \times 1.45 \times (1-\alpha) \times [-\ln(1-\alpha)]^{0.31} \quad [11]$$

2. *Analysis at 933 K (660 °C): contribution to the study of stage II*

a. Effect of carbon content. The temperature was chosen to be 933 K (660 °C) in stage II of the carbochlorination reaction of europium oxide.

To analyze the influence of carbon content on the Eu_2O_3(s) carbochlorination reaction rate, the reactions were performed with different carbon percentages. The experimental conditions were T = 933 K (660 °C); PCl_2 = 35 kPa and Cl_2(g)-Ar(g) flow = 4 L h^{-1}; and $M_{0Eu_2O_3}$ = 3 mg and pct carbon = 0 to 10. The corresponding TG curves with the $\Delta M/M_{0Eu_2O_3}$ as a function of time are depicted in Figure 9. These curves indicate that the carbon content has an influence on the products and kinetics of the stage II. The inset plot in Figure 9 is a magnification of the reaction beginning (stage I); it showed independence of the reaction with the carbon content.

The XRD analyses of final products of the reactions at 933 K (660 °C) are displayed in Figure 10. For a comparison, the reference patterns of EuOCl(s) and $EuCl_3$(s) are displayed in Figure 10.[20] The hygroscopic samples were opened in a glove box to be characterized. The product of carbochlorination with 6 pct initial carbon at 933 K (660 °C) was identified as $EuCl_3$(s) by WD-XRF. Figure 11 shows an SEM image of the product, and particles of carbon partially reacted during the interaction with Cl_2(g) were observed, which are contained inside solidified $EuCl_3$(s).

The mass balances performed in the first stage, the formation of EuOCl(s), and the independence of initial carbon content are in agreement with Reaction [5].

By comparing the experimental diffractograms with the reference patterns is inferred that the reaction product is EuOCl(s) for 0 pct carbon, a mixture of EuOCl(s) and $EuCl_3$(s) for 3 pct carbon, and $EuCl_3$(s) for carbon content higher than 6 pct.

The behavior observed for the carbon content influence can be explained by taking into account the thermodynamic and kinetic effects of the sucrose carbon. The thermodynamic effect is to provide a low oxygen potential atmosphere, favoring the formation of the chloride. The kinetic effect is a result of the formation of highly reactive gas intermediates.[26–31]

If the temperature is close to the melting temperature (T_m) of $EuCl_3$ and pct C higher than stoichiometry of the carbochlorination reaction, the system advances through second stage until the complete formation of the chloride. If the temperature is lower than T_m $EuCl_3$ or the percent carbon lower than stoichiometry of reaction, a fraction of the EuOCl(s) produced through first stage is carbochlorinated forming $EuCl_3$(l) and the final product is EuOCl(s) + $EuCl_3$(l).

Figure 12 shows the infrared spectrum of the gases collected after a carbochlorination was carried out at 933 K (660 °C) in the fixed bed reactor. The experi-

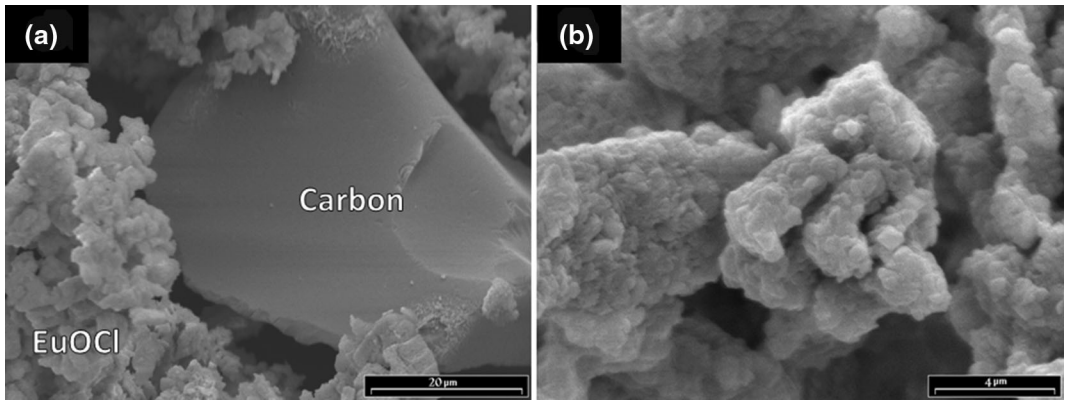

Fig. 8—SEM images of the solid residue after reaction at 673 K (400 °C): (*a*) unreacted carbon and (*b*) EuOCl(s) particles.

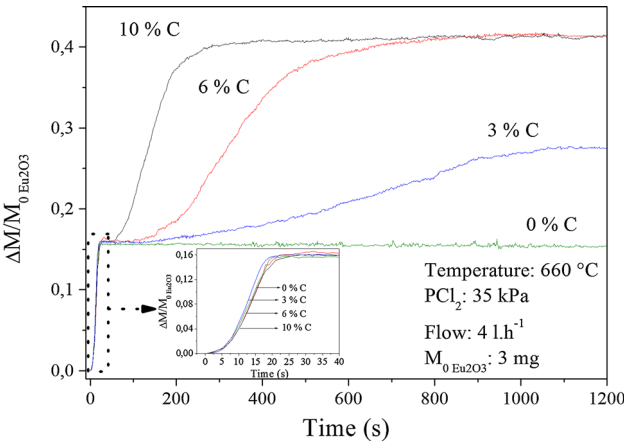

Fig. 9—Influence of carbon content in the chlorination of Eu_2O_3(s) at 933 K (660 °C). Inset plot is a magnification of the reaction beginning.

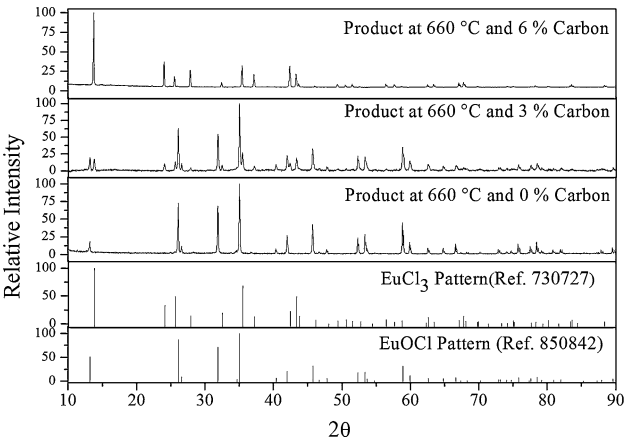

Fig. 10—XRD patterns of the products of the Eu_2O_3(s) carbochlorination with 0, 3, and 6 pct of initial carbon at 933 K (660 °C), EuOCl(s) and $EuCl_3$(s) reference.

mental conditions were PCl_2 = 101 kPa (1 atm), Cl_2(g) flow = 2 L h^{-1}, $M_{0Eu_2O_3}$ = 50 mg, and percent carbon = 6. The gas species were conducted to the cell for FTIR analysis after 120 seconds of reaction. The gases passed through the cell for 120 seconds; then the cell was

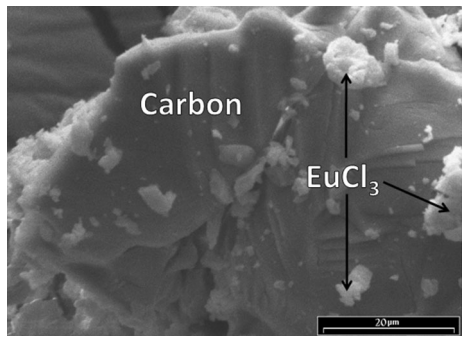

Fig. 11—SEM image of $EuCl_3$(s) produced at 933 K (660 °C).

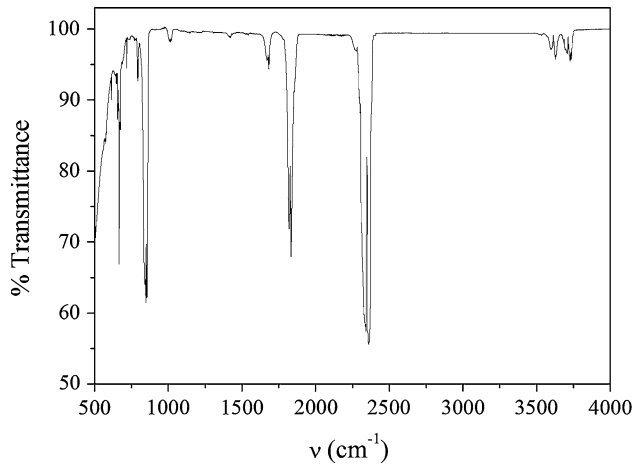

Fig. 12—Infrared spectrum of gas species generated after Eu_2O_3(s) carbochlorination at 933 K (660 °C).

isolated and afterward they were diverted to the purge. The cell was removed and analyzed by FTIR.

The FTIR spectrum revealed the presence of CO_2(g) and $COCl_2$(g). The absorption bands at 610 to 723, 2343 to 2361, and 3545 to 3760 cm^{-1} correspond to carbon dioxide and the bands at 555 to 605, 785 to 875, and 1650 to 1880 cm^{-1} belong to phosgene ($COCl_2$(g)).

The production of $COCl_2$(g) was not proposed because it was not detected in the carbochlorination reactions with sucrose carbon,[19, 26] and $COCl_2$(g) decomposes

forming CO(g) and Cl_2(g) at temperatures above 923 K (650 °C).[32] However, the reaction between Cl_2(g) and CO(g) with formation of $COCl_2$(g) may happen in the cold zones of the reactor.

Therefore, the identification of the gas products indicates that the reactions at the second stage are the Reactions [8] and [9]. In the following sections, we have studied the kinetics of the reaction of the second stage. The carbon content used was 6 pct, which allows the reaction of europium trichloride formation is complete.

b. Effect of chlorine flow rate. The overall rate in gas–solid reactions can be controlled by gas phase mass transfer by two processes: reacting gas starvation and convective mass transfer through the boundary layer. The first process can be analyzed by studying the effect of the total flow rate on the reaction rate.[33] Three different flow rates were evaluated: 2, 4, and 8 L h^{-1}. Figure 13 illustrates the effect of chlorine flow rate on the carbochlorination kinetics of Eu_2O_3(s) at 933 K (660 °C). The experimental conditions were PCl_2 = 35 kPa and percent carbon = 6. It can be concluded that the supply rate of chlorine is not influencing the kinetics parameters of second stage at this temperature.

c. Effect of initial sample mass. Figure 14 shows the effect of the sample mass between 1 and 20 mg in carbochlorinations performed at 888 K and 933 K (615 °C and 660 °C) with the following experimental conditions: PCl_2 = 35 kPa, Cl_2(g)-Ar(g) flow = 4 L h^{-1}, and percent carbon = 6. The thermogravimetric curves show that the reaction kinetics depends on the sample mass. It can be seen that the reaction rate becomes faster as the starting mass sample increases from 1 to 20 mg. This behavior is not the most common in gas–solid reaction kinetics. An increment in the reaction thickness bed generally causes the following, depending on the importance of the diffusion through the sample pores: (1) a diminution in the reaction rate for systems affected by this diffusion or (2) no change in the kinetics for systems that are not influenced by this transfer process. The increase of the reaction rate with the initial mass can be related to the formation of *highly reactive gas intermediates*, in which chlorine radical ($Cl^{\cdot}$) is the most probable to be formed in the Cl_2(g)-C(s) interaction.[26,27,31] As the reaction thickness of the bed increases, the reaction probability before the recombination to form Cl_2(g) increases. When the reaction thickness diminishes, the chlorine radicals have a higher probability of escaping from the sample and do not interact with the oxychloride and carbon.

Taking in consideration the preceding observations[26,27,34,35] and the results obtained in the present investigation, the mechanism of second stage is suggested to be as follows:

- Activation of chlorine on the carbon surface:

$$Cl_2(g) + C(s) = 2Cl^{\cdot}(g) + C(s) \qquad [12]$$

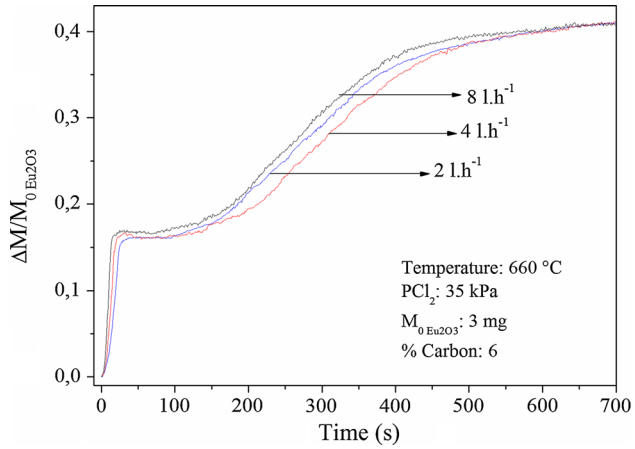

Fig. 13—Influence of gaseous flow rate in the carbochlorination of Eu_2O_3(s) at 933 K (660 °C).

- Chlorination of europium oxychloride by the active species $Cl^{\cdot}$(g):

$$EuOCl(s) + 2Cl^{\cdot}(g) = EuCl_3(l) + 1/2O_2(g) \qquad [13]$$

- Carbon oxidation:

$$1/2O_2(g) + 1/2C(s) = 1/2CO_2(g) \qquad [14]$$

$$1/2O_2(g) + C(s) = CO(g) \qquad [15]$$

To analyze the effect of temperature and chlorine partial pressure on the Eu_2O_3(s) carbochlorination rates, initial mass of 3 mg was chosen because the two carbochlorination stages are well differentiated.

C. *Determination of the Rate Equation for the Formation of $EuCl_3$(l) (Stage II)*

Usually, the rate of a heterogeneous solid–gas reaction can be written, assuming separability of variables, as:[36]

$$\frac{d\alpha}{dt} = K(T) \cdot F(PCl_2) \cdot G(\alpha) \qquad [16]$$

In Eq. [16], $G(\alpha)$ is a function that describes the geometric evolution of the reacting solid, $K(T)$ refers to an Arrhenius equation, and $F(PCl_2)$ expresses the dependence of the reaction rate with the gaseous reactant.

In the present case, the mass change measured in the thermobalance includes the weights of Eu_2O_3(s) and EuOCl(s) at the first stage and of EuOCl(s) and $EuCl_3$(l) at the second stage, taking as second stage initial mass the EuOCl(s) formed in carbochlorination in first stage, and the $\Delta M/M_{0Eu_2O_3}$ observed in the thermogravimetry,

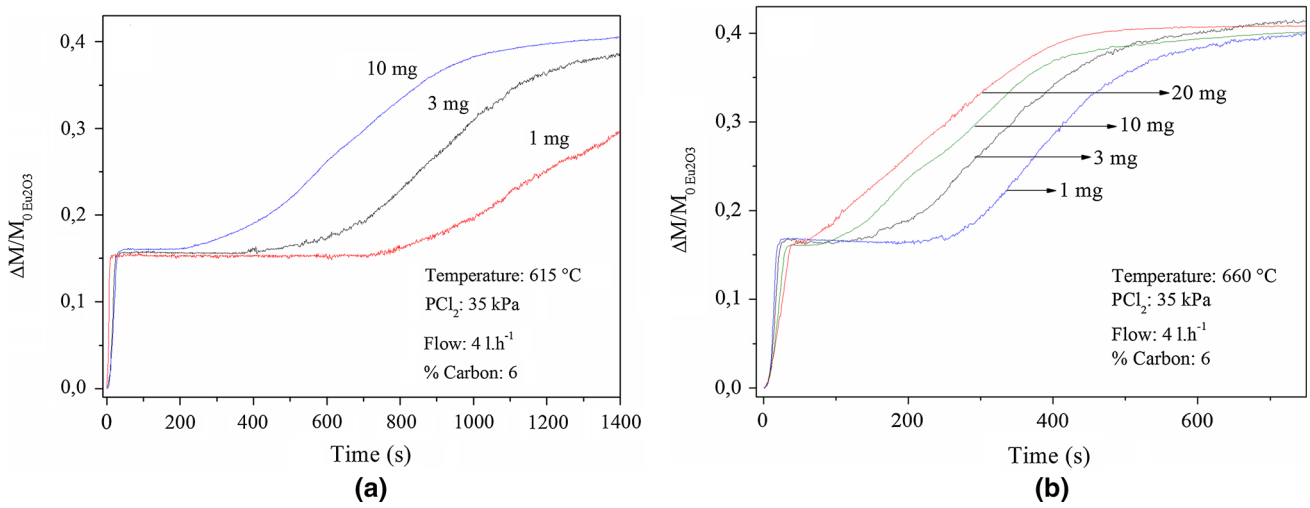

Fig. 14—Influence of initial sample mass in the carbochlorination of Eu_2O_3(s) at (*a*) 888 K (615 °C) and (*b*) 933 K (660 °C).

Table I. Calculated and Experimental Cl_2(g) Molar Transfer Rates

Temperature [K (°C)]	$N_{calculated}$ (mol Cl_2 s^{-1}), N_C	$N_{experimental}$ (mol Cl_2 s^{-1}), N_E	N_C/N_E
888 (615)	6.1×10^{-6}	2.54×10^{-8}	240.2
903 (630)	6.1×10^{-6}	3.56×10^{-8}	171.3
918 (645)	6.2×10^{-6}	3.74×10^{-8}	165.8
933 (660)	6.3×10^{-6}	4.56×10^{-8}	138.2
943 (670)	6.5×10^{-6}	4.91×10^{-7}	64.7

the degree of conversion of the second stage is defined as:

$$\alpha = \left(\frac{\Delta M}{M_{0Eu_2O_3}} \cdot 4.27\right) - 0.66. \qquad [17]$$

1. *The Ranz-Marshall correlation*

The influence of the mass transfer through the boundary layer surrounding the solid sample on the reaction rate was analyzed between [888 and 943 K (615 and 670 °C)] by comparing the experimental rate (N_E) with the rate of chlorine diffusion calculated (N_C) by using the Ranz-Marshall correlation.[37]

The calculation of N_C and the determination of N_E were carried out through the same procedure as detailed in the work *Kinetic Study of Europium Oxide Chlorination*.[18]

Table I shows the values of N for PCl_2 = 35 kPa, Cl_2(g)-Ar(g) flow = 4 L h^{-1}, $M_{0Eu_2O_3}$ = 3 mg, percent carbon = 6, and several temperatures.

In the temperature range between [873 K and 933 K (600 °C and 660 °C)], the binary diffusion coefficient can be expressed by: D_{Cl_2-Ar} (cm^2 s^{-1}) = –0.14 + 1.5×10^{-3} T.[38]

When the experimental rate is in the order of the calculated value, it can be concluded that the mass transfer influences the reaction kinetics. On the opposite, when the experimental rate is two or more orders of magnitude smaller than the calculated value, the reaction rate is not affected by mass transfer in the gas phase. In the case of reaction under diffusion control, the interfacial reaction rate will be so fast that the reaction rate will be controlled by diffusion through the boundary layer; then, the experimental values N_E will tend to the calculation values.[18] For these reasons, the experimental values cannot be greater than the calculated values. As can be seen in Table I, the experimental rates at 933 K (660 °C) and lower temperatures are two or more orders of magnitude smaller than N_C. These results indicate that at $T \leq 933$ K (660 °C), the convective mass transfer through the boundary layer is not the rate-controlling step.

2. *Effect of chlorine partial pressure*

The influence of PCl_2 on the second stage kinetics was analyzed at 933 K (660 °C) varying the partial pressures of Cl_2(g) between 20 and 70 kPa with 3 mg of Eu_2O_3(s) in the initial mixture and 6 pct carbon. Figure 15 shows the curves of conversion degree *vs* $time_{II}$, where $time_{II}$ is defined considering the starting time of the second stage as the end time of the first stage. To calculate the order of the reaction with respect to PCl_2, Eq. [16] was integrated; $F(PCl_2)$ was assumed as $B \cdot PCl_2^x$ (where B is a constant and x is the reaction order with respect to the chlorine partial pressure). From the slope of the straight lines of the $-\ln t_{II}$ *vs* PCl_2 plot for different conversion degrees, is obtained the reaction order x (Figure 15 inset shows these plots). It was found that the carbochlorination second stage rate was proportional to a potential function of chlorine partial pressure, whose exponent x is 0.56. This reaction order

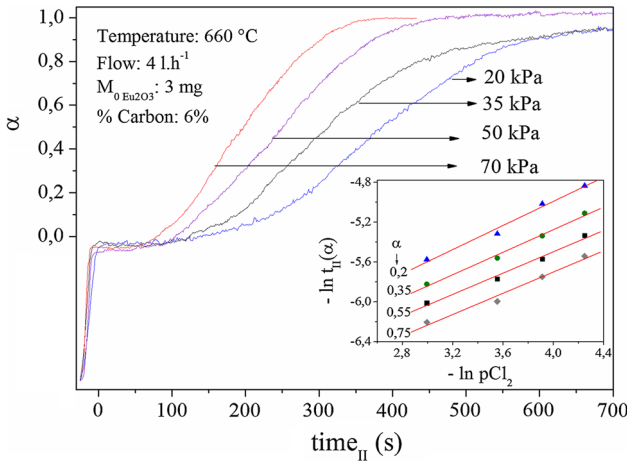

Fig. 15—Influence of pressure of $Cl_2(g)$ on the carbochlorination of $Eu_2O_3(s)$ at 933 K (660 °C). $Time_{II}$ is defined considering the starting time of the second stage as initial time.

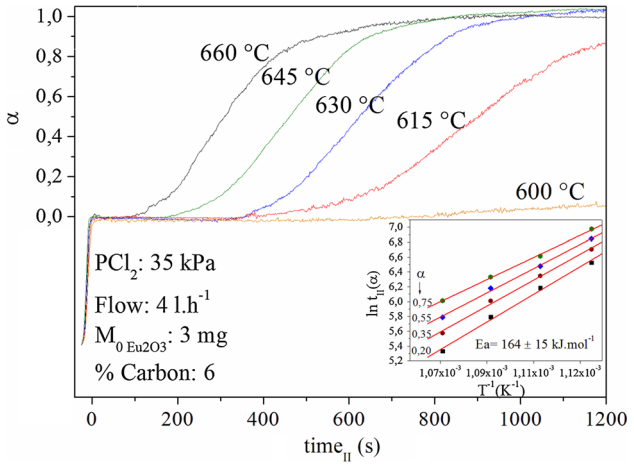

Fig. 16—Conversion degree *vs* $time_{II}$ for temperatures between [873 K and 933 K (600 °C and 660 °C)].

is close to 1/2, which could be attributed to the formation of two chlorine radicals ($Cl^{\cdot}$) from a chlorine molecule, the slow step of the mechanism suggested previously (Reaction [12]).

3. *Effect of temperature-activation energy*

Figure 16 illustrates the effect of temperature on the carbochlorination of 3 mg of $Eu_2O_3(s)$ at PCl_2 = 35 kPa, $Cl_2(g)$-Ar(g) flow = 4 L h^{-1} and percent carbon = 6. These curves indicate that the second stage rate of the carbochlorination reaction is increased as the temperature is raised, and if the temperature is 873 K (600 °C), then the final product is EuOCl(s) and the second stage does not occur.

The apparent activation energy (E_a) of the second stage was calculated using the "model-free"[39,40] method: Equation [16] is integrated, $K(T)$ is assumed that follows an Arrhenius form, PCl_2 is a constant value, and natural logarithms are applied:

$$\ln\, t_{IIi} = \ln\left[\frac{g(\alpha_i)}{F(PCl_2)\cdot K_0}\right] + \frac{E_a}{R_g\cdot T} = \text{cte} + \left(\frac{E_a}{R_g}\right)\cdot\frac{1}{T} \qquad [18]$$

where t_{IIi} is the time at which the reaction reaches a conversion degree at a temperature T and R_g is the universal gas constant. Therefore, if the chlorine partial pressure remains constant, and the time to attain a certain reaction degree is determined as a function of temperature, Eq. [18] allows to obtain the activation energy from the slope of the plot ln t_{II} *vs* T^{-1}.

Figure 16 inset shows a plot of ln t_{II} *vs* T^{-1} for α = 0.2, 0.35, 0.55, and 0.75. E_a is calculated through the slope of the curve for each α value.

The fit straight lines are practically parallels for every conversion value; this behavior is indicating that the controlling mechanism is the same at all conversions analyzed. The value obtained for E_a was 164 ± 15 kJ/mol.

The increase in the reaction rate with temperature can be attributed to the increase in the activity of the carbon surface with temperature. The higher the temperature, the higher the activity; *i.e.*, the higher the energy state of active surface atoms of carbon, the lower can be the kinetic energy of the chlorine molecules hitting the surface and causing Reaction [12].

4. *Reaction model-determination of G(α)*

The sigmoidal shape of the thermogravimetric curves is characteristic of a "nucleation and growth reaction mechanism." The conversion curves were fitted according with the Avrami-Erofeev model,[41,42] as follows:

$$\alpha = 1 - \exp(-[k(T)\cdot t_{II}]^n), \qquad [19]$$

$$k(T) = k_0\cdot\exp\left(-\frac{E_a}{R_g\cdot T}\right). \qquad [20]$$

where $k(T)$ is the global rate constant (different from $K(T)$ in Eq. [16]), k_0 is the preexponential factor, E_a is the effective activation energy, and n is the Avrami exponent. The parameters k_0, E_a, and n depend on the nucleation and growth mechanisms. Table II summarizes the values of the parameter n which may be obtained for various boundary conditions.[42]

The conversion curves of Figure 16 were fitted with Eq. [19], and Table III shows the values of n, $k(T)$, and correlation coefficient R obtained from a nonlinear least squares fitting.

Figure 17 shows the experimental curves (line graphs) and the fitted curves (scatter graphs), showing the good fit between them. The average value of n obtained was 3.8 ± 0.6. This value for n is consistent with a three-dimensional growth and phase boundary controlled.

The apparent activation energy in the temperature range of [888 K to 933 K (615 °C to 660 °C)] was calculated from the values of the global rate constant $k(T)$. Figure 18 shows the plot of ln k *vs* T^{-1}, from which a value for the apparent activation energy of 154 ± 5 kJ mol^{-1} was obtained. This value is similar to the activation energy calculated by the "model-free" method.

Table II. Values of *n* for Combination of the Different Nucleation and Growth Models

Kinetic Model	Phase Boundary Controlled	Diffusion Controlled
Three-dimensional growth	4	2.5
Two-dimensional growth	3	2
One-dimensional growth	2	1.5

Table III. Values of Parameters *n* and *k*(*T*) Obtained from the Fits of Conversion Curves with the Avrami-Erofeev Model

T [K (°C)]	$k(T)$ (seg^{-1})	*n*	Correlation Coefficient *R*
888 (615)	1.02×10^{-3}	4.25	0.9987
903 (630)	1.46×10^{-3}	4.30	0.9987
918 (645)	1.96×10^{-3}	3.64	0.9998
933 (660)	2.82×10^{-3}	3.00	0.9990

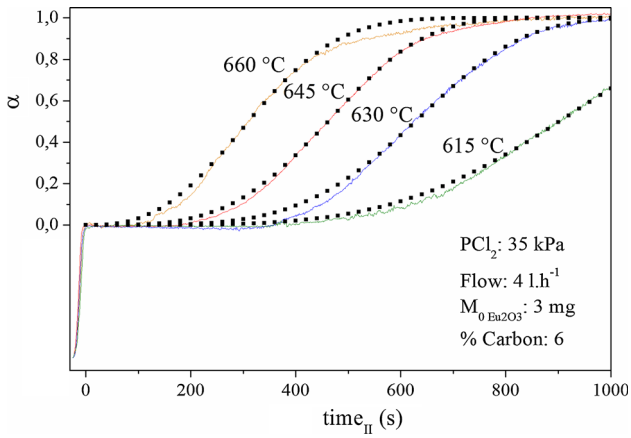

Fig. 17—Fits of the conversion curves with Avrami-Erofeev model. Line graphs: experimental curves; scatter graphs: calculated curves.

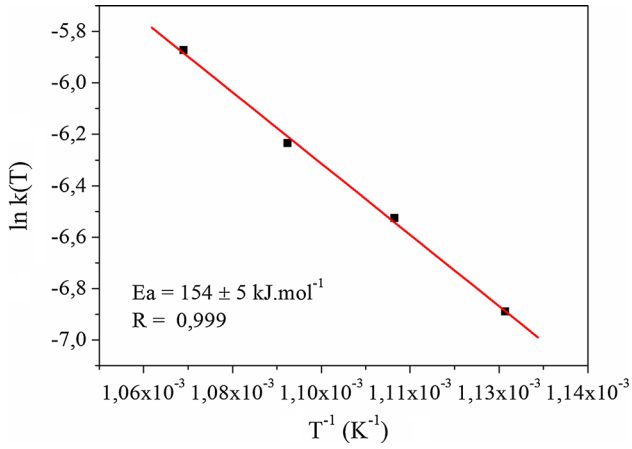

Fig. 18—ln $k(T)$ *vs* T^{-1} plot for the calculation of apparent activation energy (E_a).

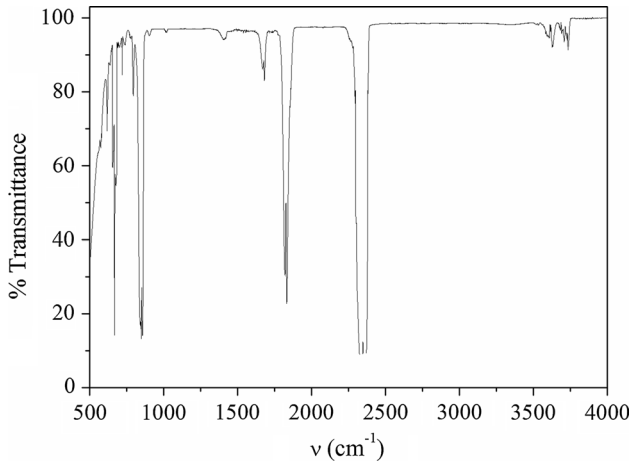

Fig. 19—Infrared spectrum of gases species of Eu_2O_3(s) carbochlorination at 1173 K (900 °C).

An overall rate equation was obtained, which includes the effects of the parameters analyzed (preexponential factor was obtained for each temperature by combining Eqs. [16], [19], and [20], and calculating the average value):

$$\text{Rate}\left[s^{-1}\right] = \frac{d\alpha}{dt} = 1.5 \times 10^5 \left[s \cdot kPa^{0.56}\right]^{-1} \times e^{-(154\,kJ\,mol^{-1})/RT} \times (PCl_2[kPa])^{0.56} \times 3.8 \times (1-\alpha) \times [-\ln(1-\alpha)]^{0.74}. \quad [21]$$

D. *Final Remarks Regarding Stage III [T > 943 K (670 °C)]*

The nonisothermal thermogravimetry of the Eu_2O_3 carbochlorination (Figure 5) showed that for temperatures above 943 K (670 °C) is observed a mass gain corresponding to the formation of liquid $EuCl_3$, and afterward a mass loss which corresponds to the evaporation of the chloride. The XRD analysis confirmed that the final condensed product of the reaction at 1173 K (900 °C) and 6 pct C is $EuCl_3$.

The identification of gas products of the reaction of $EuCl_3$ production at 1173 K (900 °C) was performed by FTIR. The experimental conditions used in the fixed bed reactor were as follows: PCl_2 = 101 kPa (1 atm), Cl_2(g) flow = 2 L h^{-1}, $M_{0Eu_2O_3}$ = 50 mg, and percent carbon = 6. The gases at the outlet of the reactor were conducted to the FTIR cell during the initial 60 seconds of reaction, and they were subsequently diverted to the purge. The FTIR absorption spectrum showed in Figure 19 has the same absorption bands than the spectrum of Figure 12, revealing the presence of CO_2(g) and $COCl_2$(g). Therefore, the identification of the gas products is indicating that at 1173 K (900 °C) the Stage II of the Eu_2O_3 carbochlorination proceeds by Reactions [8] and [9].

The Boudouard reaction is an endothermic reaction in which CO_2(g) reacts with carbon producing CO(g). This reaction is favored by high temperature; however, the

analysis by FTIR shows that the relations of $CO_2(g)$ and CO(g) are not affected by the increase of the temperature, and the thermodynamic predictions are not observed experimentally.

V. CONCLUSIONS

The $Eu_2O_3(s)$-C(s)-$Cl_2(g)$ system was analyzed in the temperature range from room temperature to 1223 K (950 °C). The results showed that the reaction proceeds through three stages.

The reaction product in the first stage is EuOCl(s). This reaction occurs for temperatures higher than 523 K (250 °C), and the kinetics do not change with the addition of sucrose carbon to the starting $Eu_2O_3(s)$.

The second stage begins at temperatures higher than 873 K (600 °C), such that the reaction product at 933 K (660 °C) varies according to the percent carbon; $EuCl_3(l)$ is the only final product when the content exceeds 6 pct.

The identification by FTIR of the gas products in the second stage was performed at [933 K and 1173 K (660 °C and 900 °C)]. The interpretation of the results showed that both CO(g) and $CO_2(g)$ are formed during the carbochlorination reaction. This behavior is not the expected by the thermodynamic calculations.

The evaporation of the $EuCl_3(l)$ is observed in the third stage for temperatures higher than 943 K (670 °C).

The reactions for the three stages in the $Eu_2O_3(s)$ carbochlorination are:

$$\text{Stage I: } Eu_2O_3(s) + Cl_2(g) + C(s) \rightarrow 2EuOCl(s) + 1/2O_2(g) + C(s) \quad [T > 523\ \text{K}\ (250\ ^\circ\text{C})]$$

$$\text{Stage II: } EuOCl(s) + Cl_2(g) + 1/2C(s) \rightarrow EuCl_3(s,l) + 1/2CO_2(g)$$

$$EuOCl(s) + Cl_2(g) + C(s) \rightarrow EuCl_3(s,l) + CO(g) \quad [T > 873\ \text{K}\ (600\ ^\circ\text{C})]$$

$$\text{Stage III: } EuCl_3(l) \rightarrow EuCl_3(g) \quad [T > 943\ \text{K}\ (670\ ^\circ\text{C})]$$

The influences of the parameters that affect the kinetics of stage II were analyzed. The reaction order with respect to the chlorine partial pressure was 0.56. Conversion curves *vs* time were analyzed with the description of Avrami-Erofeev for nucleation and growth mechanisms. Avrami-Erofeev parameters obtained were $n = 3.8 \pm 0.6$ and $E_a = 154 \pm 5$ kJ mol^{-1} in the temperature range of [888 K to 933 K (615 °C to 660 °C)].

Finally, it was obtained an overall rate equation of the carbochlorination stage II:

$$\text{Rate}\left[\text{s}^{-1}\right] = \frac{d\alpha}{dt} = 1.5 \times 10^5 \left[\text{s} \cdot \text{kPa}^{0.56}\right]^{-1} \times e^{-(154\text{kJ}\cdot\text{mol}^{-1})/RT} \times \left(PCl_2[\text{kPa}]\right)^{0.56} \times 3.8 \times (1-\alpha) \times \left[-\ln(1-\alpha)\right]^{0.74}$$

It was observed that the kinetics of the second stage show an anomalous behavior respect to the variation of the reaction bed thickness. An increase of the sample initial mass and the carbon content leads to an increment of the reaction rate. This behavior can be explained by the generation of highly reactive intermediate species, such as chlorine radicals ($Cl^{\cdot}$) produced during the interaction of $Cl_2(g)$ with carbon.

ACKNOWLEDGMENTS

The authors thank the Consejo Nacional de Investigaciones Científicas y Técnicas (CONICET), Universidad Nacional del Comahue, and Agencia Nacional de Promoción Científica y Tecnológica (ANPCyT) for the financial support of this work.

REFERENCES

1. C.K. Gupta and N. Krishnamurthy: *Extractive Metallurgy of Rare Earths,* CRC Press, London, U.K., 2005, pp. 27–31, 151–2.
2. Z.C. Wang, L.Q. Zhang, P.X. Lei, and M.Y. Chi: *Metall. Mater. Trans. B*, 2002, vol. 33B, pp. 661–68.
3. L.Q. Zhang, Z.C. Wang, S.X. Tong, P.X. Lei, and W.Z. Wei: *Metall Mater. Trans. B*, 2004, vol. 35B, pp. 217–21.
4. N. Kanari, E. Allain, R. Joussemet, J. Mochón, I. Ruiz-Bustinza, and I. Gaballah: *Thermochim. Acta*, 2009, vol. 495, pp. 42–50.
5. C.-H. Kim, S.I. Woo, and S.H. Jeon: *Ind. Eng. Chem. Res.*, 2000, vol. 39 (5), pp. 1185–92.
6. J.A. Sommers: U.S. Patent US5569440 A, 1994.
7. Y. Mochizuki, N. Tsubouchi, and K. Sugawara: *ACS Sust. Chem. Eng.*, 2013, vol. 1 (6), 3, pp. 655–62.
8. F. Habashi: *Handbook of Extractive Metallurgy*, Wiley, New York, NY, 1997.
9. W. Kroll: *Trends Electrochem. Soc.*, 1940, vol. 78, pp. 35–47.
10. J.P. Gaviría and A.E. Bohé: *Thermochim. Acta*, 2010, vol. 509, pp. 100–10.
11. J.P. Gaviría, G.G. Fouga, and A.E. Bohé: *Thermochim. Acta*, 2011, vol. 517, pp. 24–33.
12. W Brugger and E Greinacher: *J. Met.*, 1967, vol. 19, pp. 32–35.
13. M.A. Gimenes and H.P. Oliveira: *Metall. Mater. Trans. B*, 2001, vol. 32B, pp. 1007–13.
14. T. Ozaki, J. Jiang, K. Murase, K. Machida, and G. Adachi: *J. Alloy. Compd.*, 1998, vol. 265, pp. 125–31.
15. K. Murase, T. Fukami, K. Machida, and G. Adachi: *Ind. Eng. Chem. Res.*, 1995, vol. 34, pp. 3963–69.
16. M.R. Esquivel, A.E. Bohé, and D.M. Pasquevich: *Thermochim. Acta*, 2003, vol. 403, pp. 207–78.
17. M.R. Esquivel, A.E. Bohé, and D.M. Pasquevich: *Trans. Inst. Min. Metall. (Sect. C: Miner. Process. Extract. Metall.),* 2002, vol. 111, pp. C149–C55.
18. F.J. Pomiro, G.G. Fouga, and A.E. Bohé: *Metall. Mater. Trans. B*, 2013, vol. 44B, pp. 1509–19.
19. J. Gonzalez, M.C. Ruiz, A.E. Bohé, and D.M. Pasquevich: *Carbon*, 1999, vol. 37, pp. 1979–88.
20. Joint Committee for Powder Diffraction Standards: *Powder Diffraction File*, International Center for Diffraction Data, Swarthmore, PA, 1996.
21. O. Knacke, O. Kubaschewski, and K. Hesselman: *Thermochemical Properties of Inorganic Substances*, 2nd ed., Springer, Berlin, Germany, 1991, pp. 1–1113.
22. D. Brown: *Halides of the Lanthanides and Actinides*, Wiley, New York, NY, 1968, p. 117.
23. L.P. Ruzinov and B.S. Guljanickij: *Ravnovesnye Prevrasoenija Metallugiceskin Reaktseij*, Russia, Moscow, 1975, p. 416.
24. L. Rycerz and M. Gaune-Escard: *Z. Naturforsch*, 2002, vol. 57A, pp. 215–20.
25. HSC 6.12, Chemistry for Windows, Outokumpu Research Oy, Pori, Finland, 2007.
26. D.M. Pasquevich: Ph.D. Dissertation, Facultad de Ciencias Exactas de la Universidad Nacional de La Plata, Buenos Aires, Argentina, 1990.
27. I. Barin and W. Schuler: *Metall. Trans. B*, 1980, vol. 11, pp. 199–207.

28. D.M. Pasquevich, J.A. Gamboa, and A. Caneiro: *Thermochim. Acta*, 1992, vol. 29, pp. 209–22.
29. S.L. Stefanyuk and I.S. Morozov: *Z. Prikl. Khim.*, 1965, vol. 38, pp. 737–42.
30. W.E. Dunn, Jr.: *Metall. Trans. B*, 1979, vol. 10, pp. 271–77.
31. V.T. Amorebieta and A.J. Colussi: *J. Phys. Chem. Kinet.*, 1985, vol. 17, pp. 849–58.
32. O. Knacke, O. Kubaschewski, and K. Hesselman: *Thermochemical Properties of Inorganic substances*, 2nd ed., Springer, Berlin, Germany, 1991.
33. J. Szekely, J.W. Evans, and H.Y. Sohn: *Gas-Solid Reactions*, Academic Press, New York, NY, 1976.
34. M.W. Ojeda, J.B. Rivarola, and O.D. Quiroga: *Min. Eng.*, 2002, vol. 14, pp. 585–91.
35. D.M. Pasquevich and V.T. Amorieta: *Phys. Chem. Chem. Phys.*, 1992, vol. 96, pp. 534–37.
36. S.K. Kim: Ph.D. Dissertation, University of Utah, Salt Lake City, UT, 1981.
37. W.E. Ranz and W.R. Marshall, Jr.: *Chem. Eng. Prog.,* 1952, vol. 48, pp. 141–6, 173–80.
38. G.H. Geiger and D.R. Poirier: *Transport Phenomena in Metallurgy*, Addison-Wesley, Boston, MA, 1973, pp. 7–13.
39. J.H. Flynn: *J. Therm. Anal.*, 1988, vol. 34, pp. 367–81.
40. S. Vyazovkin: *Thermochim. Acta*, 2000, vol. 355, pp. 155–63.
41. T.J.W. De Bruijn, W.A. De Jong, and P.J. Van Den Berg: *Thermochim. Acta*, 1981, vol. 45, pp. 315–25.
42. A. Ortega, L. Perez Maqueda, and J.M. Criado: *Thermochim. Acta*, 1995, vol. 254, pp. 147–52.